

Developing a Conjugate Heat Transfer Solver

Mansour A. Al Qubeissi

Abstract—The current paper presents a numerical approach in solving the conjugate heat transfer problems. A numerical heat conduction code is coupled internally with a computational fluid dynamics solver for developing a coupling conjugate heat transfer solving package. Methodology of treating non-matching meshes at interface has also been introduced. The package can deal with a wide range of compressible flow conjugate heat transfer problems. The solver is also able to deal with various geometrical and thermal complexities. The validation results for the developed conjugate heat transfer code have shown close agreement with the available analytical solutions.

Keywords—Computational Fluid Dynamics, Conjugate Heat Transfer, Heat Exchanger, Heat Transfer

I. INTRODUCTION

THE increase in temperature in many industrial conjugate heat transfer systems is associated with a significant increase in power outputs and efficiencies. As a result, effective cooling is an essential feature in the design requirements. Predicting the temperature distribution profile for such domains is very important. When heat transfer occurs between two (or more) different materials, (fluid/solid mostly), boundary conditions are continuously interacting between these different domains. This operation is described as a conjugate heat transfer system. The main challenge in solving such problems is interface data interaction. Types of governing equations applied and data interacted depend on: type of domain (fluid/solid) and purpose of operating this system. This operation is processed in coupling fluid flow and heat conduction solvers. A cell vertex (vertex-centered) Finite Volume Method (FVM) is used for solving the heat conduction equation [1]. The fluid flow equations are solved numerically with a commercial computational fluid dynamics code (SURF) [2].

Treatment of non-matching interface meshes is made using linear interpolation. This method has been used by [3] and described as a simpler, well working data interaction technique. The linear interpolation technique in matching nodes has been previously applied on structured grids using the second order central difference method [4]. In unstructured meshes, transferring accurate data can be more complicated because the finite difference technique will not be valid. In addition, the sizes and shapes of the boundary elements may differ from one side to another.

M. A. al Qubeissi, a Researcher in Computational Fluid Dynamics (CFD) development at FMRC, University of Sussex, Brighton, BN1 9QT UK (Phone: 01273 87 6706; e-mail: ma292@sussex.ac.uk).

II. HEAT CONDUCTION EQUATION

HC code is developed to solve the heat conduction equation. The governing equation is solved for a control volume, shown in Fig. 1, with no internal heat generation as:

$$\rho C \frac{\partial T}{\partial t} + \bar{\nabla} \cdot \bar{q} = 0 \quad (1)$$

In (1), T is the temperature value given in (K) and ρC represent density and heat capacity with units (kg m^{-3}) & ($\text{W kg}^{-1}\text{K}^{-1}$) respectively. \bar{q} is the heat flux in three components, given by Fourier's law as:

$$\bar{q} = -k \bar{\nabla} T \quad (2)$$

The numerical solutions of (1) & (2) are further described in [1].

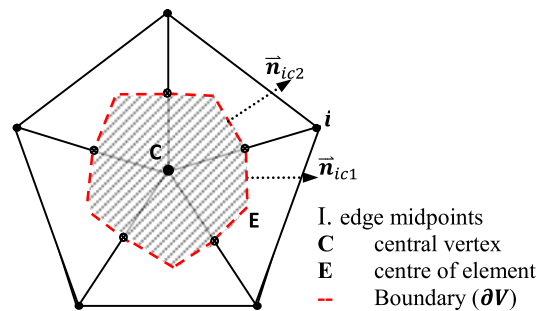


Fig. 1 2D view of the vertex centered control volume [1]

III. FLUID FLOW EQUATIONS

The fluid flow equations of Navier stokes, momentum and energy conservation are solved numerically using Spalart and Allmaras turbulent model [5]. SURF is validated, as a computational fluid dynamics tool, to deal with steady and unsteady, compressible, three dimensional flow problems [2]. The heat transfer between the solid-interface surface and the fluid layer adjacent to that interface can be assumed of pure conduction by considering the fluid in that region as motionless [6]. The thermal boundary layer thickness δ_T can be obtained in a relation with the velocity boundary layer thickness and Prandtl number [6] as:

$$\delta_T = \text{Pr} \delta_v \quad (3)$$

Where, δ_v is the velocity boundary layer thickness and Pr is Prandtl number, which is assumed for approximation as

$Pr \cong 0.697$ when air flow in a channel of higher temperature than the surface and $Pr \cong 0.707$ when the channel flow is of lower temperature than the surface. The velocity boundary layer thickness, over a plane surface, δ_v can be approximated for laminar and turbulent flows [7] and [8] as:

$$\delta_v = 5.83 (Re)^{-\frac{1}{2}} ; Re \leq 2000 \quad (4)$$

$$\delta_v = 0.379 x (Re)^{-\frac{1}{5}} ; Re \gg 2000 \quad (5)$$

Where, x is the length of channel and Re is Reynolds number. Also, in laminar flow inside pipes, this thickness can be approximated as:

$$\delta_v = 0.5 D_h \quad (6)$$

Where, D_h is the characteristic length (hydraulic diameter).

IV. INTERFACE TREATMENT

Research studies [4], [9] and [10] have described the only physical requirements for a heat transfer interface interaction as: Energy conservation and Temperature continuity across interface. Applying these two conditions on both (fluid/solid) domains in one equation can be difficult when dealing with unstructured grids. However, the condition of energy and temperature continuities at interface can be applied on each domain boundary differently. This method was proved as a very successful approach of coupling [3], which can be described with two steps: First (Fluid side): Continuity of temperature along interface applied to the fluid part, i.e. Dirichlet boundary condition.

$$T_f = T_w \quad (7)$$

Second (Solid side): Continuity of heat flux, applied to the solid part, i.e.:

$$q_s = q_f \quad (8)$$

Heat fluxes, normal to the interfacial surface, are balanced from both sides at each interfacial solid node. On the other side, temperature continuity (from solid to fluid boundaries) is applied at each interfacial fluid node. In most applications, boundary elements sizes, shapes and therefore numbers of nodes from both sides may differ. The case of non-conforming meshes at interface is very common. Example of this is solved in present paper and shown in Fig. 2. The gross heat flux from one boundary to its neighbour will therefore be different. When boundary meshes are non-conforming at interface; interpolation of heat flux and temperature is needed. The nodes included in the interpolation are found by mapping

the opposite boundary within a radius of the largest element size as shown in Fig. 3. Heat flux leaving the fluid boundary towards solid domain can be determined within the boundary layer by Fourier law (2) when zeroing the velocity terms of the fluid energy equation [10] as:

$$\vec{q}_f = -k_f \nabla T_f \quad (9)$$

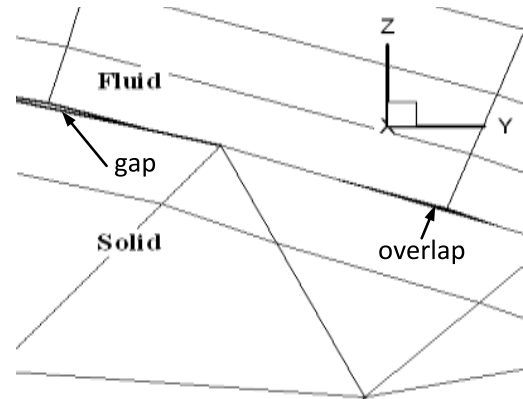


Fig. 2 The mesh of the 2D validated case in current paper showing non-conforming overlapping interface meshes

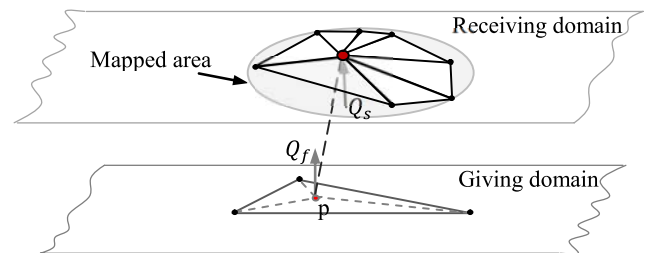


Fig. 3 Interpolation between a cell-centred-node and nearest opposite boundary element

Heat rate arriving at the solid boundary is the product of surface area weights and the heat flux received from fluid domain [11] as: $Q_s = \vec{q}_f \cdot \vec{A}_s$. The operation of giving and receiving boundary data (data interaction) is repeated with iterations. The solution convergence is been checked by assuring that the difference between the total integrated heat rates of both interface boundaries is within an acceptable tolerance as:

$$\sum_{i=1}^{N_s} Q_s - \sum_{i=1}^{N_f} Q_f \approx 0 \quad (10)$$

V. VALIDATION CASES

At the current stage of the research progress, the validations of the couple on 3 cases of 1D, of square area and round area (pipe) channel flows, and 2D case, of a pipe in square shape, are presented in the following sections. The proposed methodology, given in previous sections, is solved numerically and applied for comparison with the analytical solution. The mesh generated for each domain is in a difference size and type, which assures overlapping and non-conforming interface-grids, as shown in Fig. 3.

A. 1D case-1

A 1D fluid flow and heat conduction case of a conjugate heat transfer system is generated to test the demonstrated method of coupling. The solid part is a plate of $(1 \times 10 \times 10 \text{ m}^3)$ attached to the base $10 \times 10 \text{ m}^2$ of the channel flow with a cross section height of (3 m). The fluid flow is of 400 K temperature and $0.04 \text{ W m}^{-1} \text{ K}^{-1}$ thermal conductivity. The solid domain has a fixed wall temperature of 400 K on the downstream surface and receives heat flux from the upstream surface, which is in contact with the fluid domain, as shown in Fig. 3.

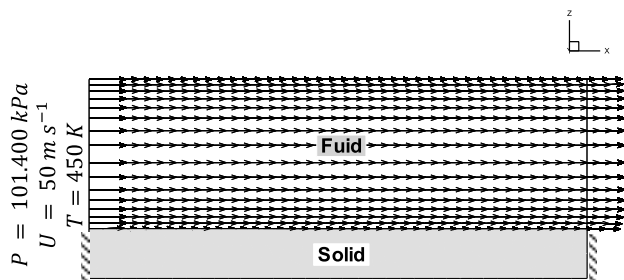


Fig. 3 Case specifications of the 1D conjugate heat transfer problem

The fluid domain is meshed with structured grids of 26800 nodes, whereas unstructured tetrahedral mesh is used for the solid domain with 11500 nodes. This assures non-conforming grids at the interface of both domains. The analytical solution of this case can be determined by substituting (8) into (9):

$$-k_s \frac{\partial T_s}{\partial y} = -k_f \frac{\partial T_f}{\partial T} \text{ yields } 10 \frac{T_s - 400}{1} = 0.04 \frac{450 - T_s}{\delta_T}$$

From (3) and (5), $\delta_T \cong 0.001 \text{ m}$. Hence, the interface temperature can be found as $T_s \cong 440 \text{ K}$ and the heat flux as $q_f = 400 \text{ W m}^{-2}$. The results given by HC-SURF couple shows good agreement with the analytical solution as illustrated in the Figs. of 8a and 8b.

B. 2D case-1

The 2D conjugate heat transfer example, shown in Fig. 5, is a hot air flow in a pipe of 0.4 m diameter. The pipe is buried 1 m inside a square section fill of construction material with dimensions of $2 \text{ m} \times 2 \text{ m}$. The cube material is of thermal conductivity $k_s = 10 \text{ W m}^{-1} \text{ K}^{-1}$ and fixed outside boundary temperatures $T = 400 \text{ K}$. The air thermal conductivity is $k_f = 0.04 \text{ W m}^{-1} \text{ K}^{-1}$.

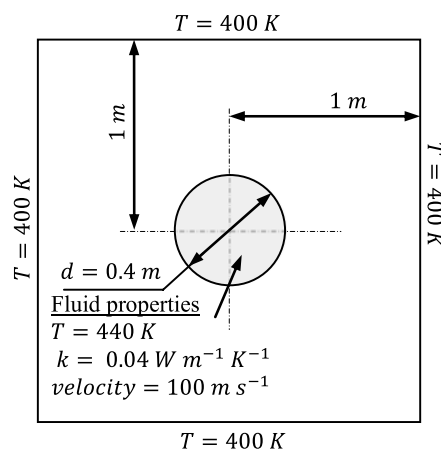


Fig. 5 An approximate dimension scale of the 2D conjugate heat transfer problem

The depth of the fill and the pipe are assumed to be unity. The heat transfer analytical solution of this case can be determined by finding the boundary layer thickness of the flow. The velocity boundary layer thickness given in (5) is $\delta_v \cong 0.006 \text{ m}$, as shown in Fig. 6. This gives the thermal boundary layer thickness of $\delta_T \cong 0.0042 \text{ m}$ as given in (3). Calling (9), the fluid flow conduction heat flux is given by: $\vec{q}_f = -k_f \frac{\partial T_f}{\partial T}$. Also from (8), the interface temperature (seen from both domains) can be found as:

$$-k_s \frac{\partial T_s}{\partial y} = -k_f \frac{\partial T_f}{\partial T} \text{ yields } 10 \frac{T_s - 400}{0.8} = 0.04 \frac{440 - T_s}{0.0042}$$

This gives the interface temperature of $T_s \cong 417 \text{ K}$ and $\vec{q}_f \cong 215 \text{ W m}^{-2}$. The numerical solution given by the HC-SURF couple gives $T_s \cong 416 \text{ K}$, similarly $\vec{q}_f \cong 200 \text{ W m}^{-2}$. The boundary layer thickness, given in [4], is an approximate average value because it may vary at different locations. Hence, the heat flux is also an estimated average value of the local ones. It is worth mentioning that a coarse grid is used for the solid domain of 4450 nodes and a relatively average density structured grid is employed for the fluid domain with about 7700 nodes. The numerical solution results provided by SURF-HC couple are illustrated in diagrams of Figs. 9a-9b.

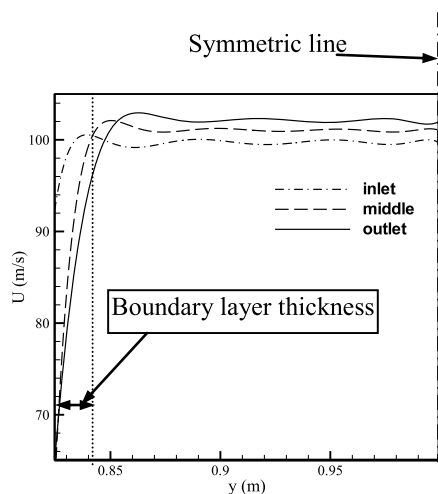


Fig. 6 Velocity profile of the air flow in a quarter of the pipe showing the average boundary layer thickness

C. 2D case-2

A high pressure double-pipe heat exchanger of inner-pipe and outer-pipe diameters 0.3 mm and 0.64 mm, respectively. The inner pipe thickness is 0.07 mm, i.e. 0.44 mm in diameter, as shown in Fig. 7.

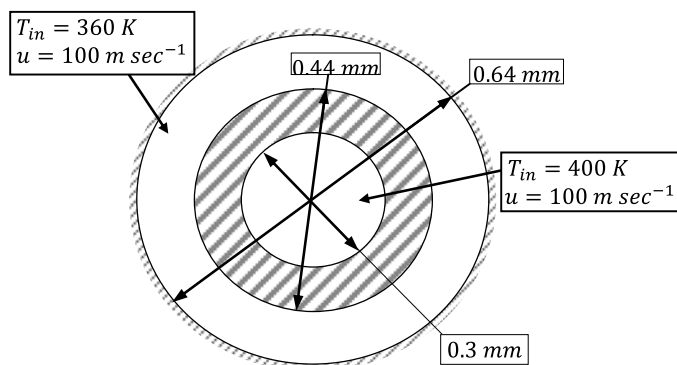


Fig. 7 An approximate dimension scale of the concurrent heat exchanger

This system is wrapped with a perfect insulation. The air velocity inside both pipes are of the same values, $u = 100 \text{ m sec}^{-1}$; whereas inlet temperatures at entrance are: in the inner pipe $T_{in} = 360 \text{ K}$ and in the outer pipe $T_{in} = 400 \text{ K}$. The thermal conductivity of the inner pipe (Steel/Nickel Ni40%), between both micro-channel flows, is $k = 10 \text{ W m}^{-1} \text{ K}^{-1}$. The flow direction in the double pipe system is tested for both concurrent and counter flows. It is worth mentioning that the system is of 80 mm in length to assure a fully developed laminar flow. The results compared to Fluent are shown in Figs. 10a-10e.

VI. CONCLUSIONS

The finite volume vertex centred scheme has been applied in discretising the heat conduction equation to examine the temperature profile of complex geometries [1]. The results, obtained from the developed codes of HC and HC-SURF couple, have been assessed with the analytical and other computational solutions upon availability. The predicted temperature profiles given by the proposed solving codes are in excellent agreement with the available standard solutions. The codes were tested to be computationally efficient; therefore, further work will involve modelling a real industrial 3D conjugate heat transfer case of rotating discs-cavities system using the conjugate heat transfer (SURF-HC) couple.

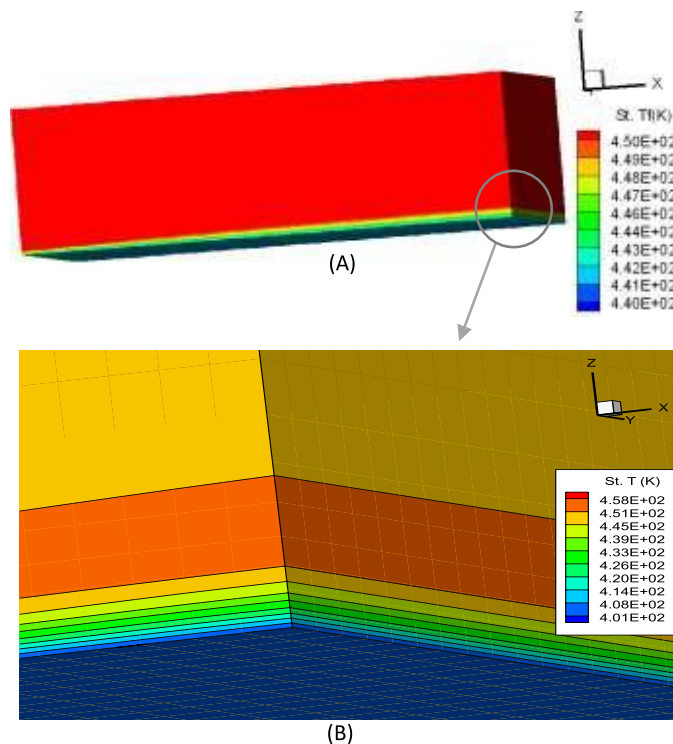


Fig. 8a Temperature contours in the fluid side: (A) complete view of the fluid geometry (B) zoom at the corner

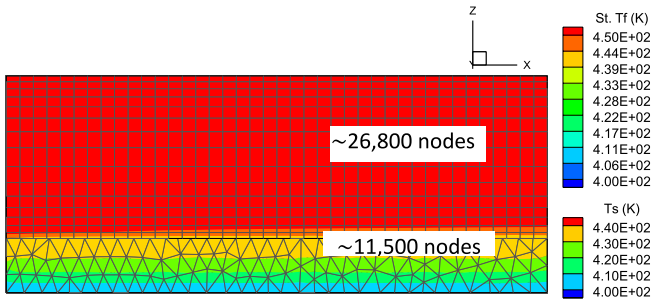


Fig. 8b Full view of the 1D conjugate heat transfer system showing the grids used and temperature profile in both domains

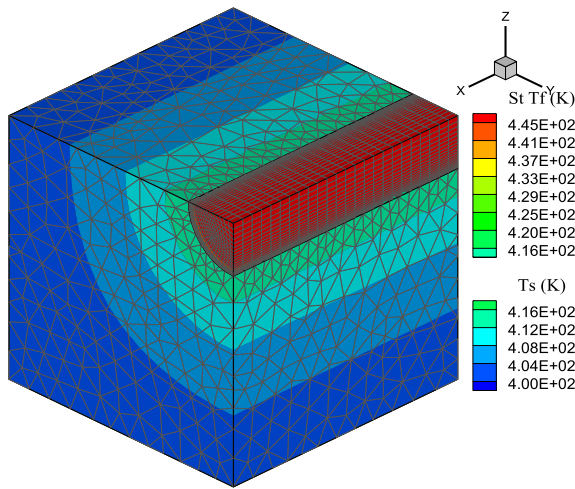


Fig. 9a 3D view of the 2D case conjugate system showing the meshes and the colour bands of temperature in both domains

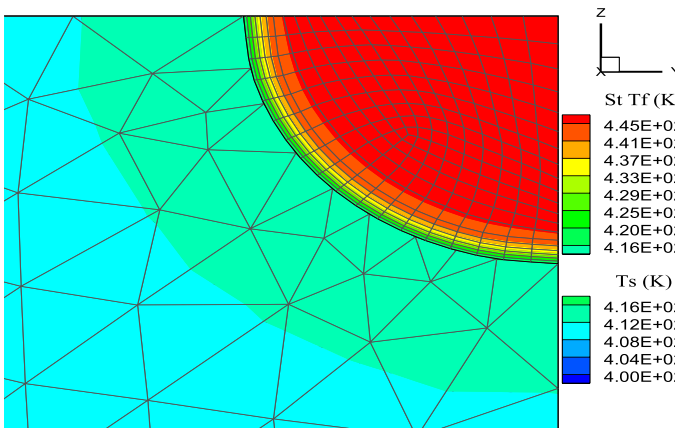


Fig. 9b Side view (yz-plane) of the 2D case showing the meshes and temperature contours

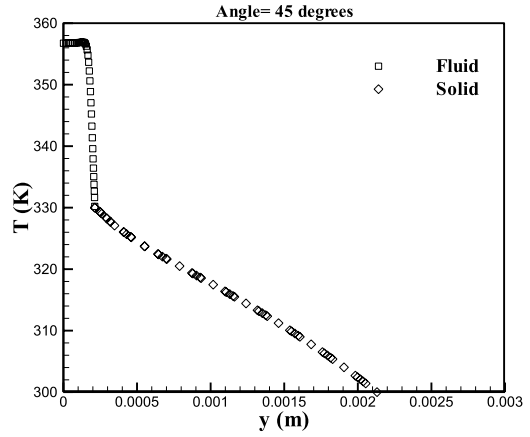


Fig. 10a Temperature profile of both domains at $x = 0.15$ mm with 45° angle from y-axis

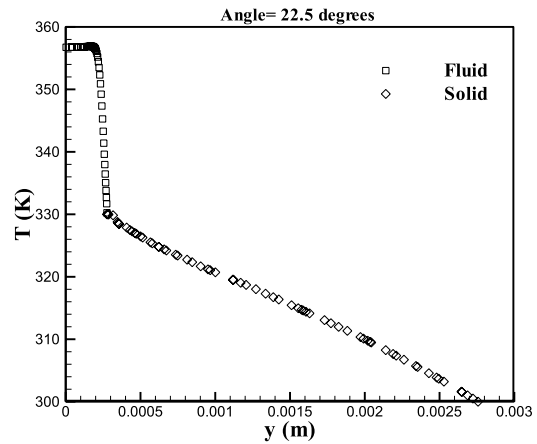


Fig. 10b Temperature profile of both domains at $x = 0.15$ mm with 22.5° angles from y-axis

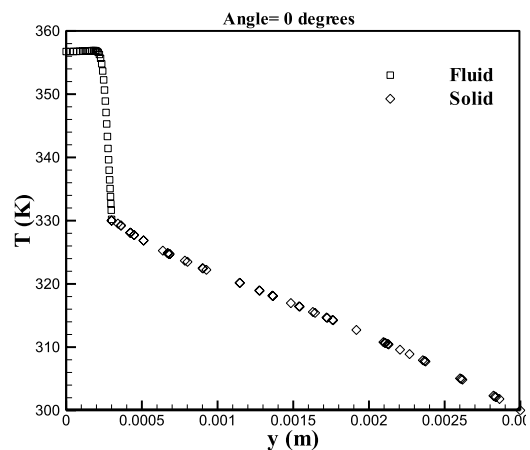


Fig. 10c Temperature profile of both domains at $x = 0.15$ mm with 0° angle from y-axis

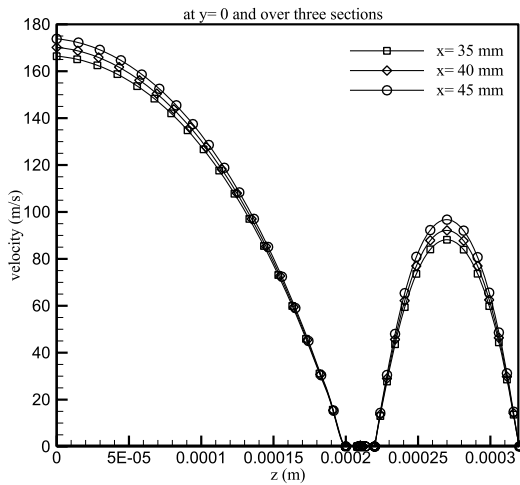


Fig. 10d Velocity profile (rings) at three sections compared to Fluent (lines)

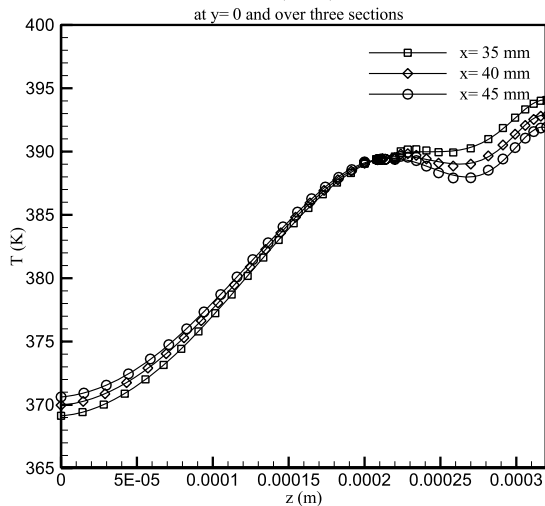


Fig. 10e Temperature profile (indicated shapes) at three sections compared to Fluent (lines)

- [8] J.M. Kay, and R.M. Nedderman (1979) An Introduction to Fluid Mechanics and Heat Transfer. 3rd Ed., Univ. Press, ISBN 0521205336.
- [9] J. Luo, and E.H. Razinsky (2007) Conjugate Heat Transfer Analysis of a Cooled Turbine Vane Using the V2F Turbulence Model. *J. Turbomach.*: 129/ 773-781.
- [10] L. He, and M.L.G. Oldfield (2010) Unsteady Conjugate Heat Transfer Modeling. *J. Turbomach.*: 133 / 031022-1.
- [11] Li, Y. and Kong, S.Ch. (2011) Coupling Conjugate Heat Transfer with in-Cylinder Combustion modelling for engine simulation. *Int. J. H. & Mass Trans.*

REFERENCES

- [1] M. Al Qubeissi (2012) Proposing a Numerical Solution for the 3D Heat Conduction Equation. *IEEE 6th Asia Int. Conf. on Math./Analyt. Model. & Comp. Sim. (AMS2012)*.
- [2] A. I Sayma, M. Vahdati, L. Sbardella, and M. Imregun (2000) Modelling of 3D viscous compressible turbomachinery flows using unstructured hybrid grids. *AIAA 38(6)*, pp 945-954.
- [3] W.D. Henshaw, and K.K. Chand (2009) A Composite Grid Solver for Conjugate Heat Transfer in Fluid-Structure Systems. *J. Comp. Phys.*
- [4] M.B. Giles (1997) Stability Analysis of Numerical Interface Conditions in Fluid-Structure Thermal Analysis. *J. Num. Meth. Fluids*: 25, 4/ 421-436.
- [5] P.R. Spallart, and S.R. Allmaras (1991) One equation Turbulence Model for Aerodynamic Flows. *AIAA*, 92-0439.
- [6] Y.A. Cengel, and R.H. Turner (2001) *Fundamentals of Thermal-Fluid Sciences*. McGraw-Hill Higher Edu, Singapore (ISBN 0-07-239054-9).
- [7] H. Schlichting, and K. Gresten (2000) *Boundary Layer Theory*, 8th Ed. Springer-Verlag Berlin, ISBN 3-540-66270-7.